

Predicting delta avulsions: Implications for coastal wetland restoration

Douglas A. Edmonds¹, David C.J.D. Hoyal², Ben A. Sheets³, and Rudy L. Slingerland¹

¹Department of Geosciences, The Pennsylvania State University, University Park, Pennsylvania 16802, USA

²Exxon Mobil Upstream Research Company, 3120 Buffalo Speedway, Houston, Texas 77098, USA

³School of Oceanography, University of Washington, Box 357940, Seattle, Washington 98195, USA

ABSTRACT

River deltas create new wetlands through a continuous cycle of delta lobe extension, avulsion, and abandonment, but the mechanics and timing of this cycle are poorly understood. Here we use physical experiments to quantitatively define one type of cycle for river-dominated deltas. The cycle begins as a distributary channel and its river mouth bar prograde basinward. Eventually the mouth bar reaches a critical size and stops prograding. The stagnated mouth bar triggers a wave of bed aggradation that moves upstream and increases overbank flows and bed shear stresses on the levees. An avulsion occurs as a time-dependent failure of the levee, where the largest average bed shear stress has been applied for the longest time ($R^2 = 0.93$). These results provide a guide for predicting the growth of intradelta lobes, which can be used to engineer the creation of new wetlands within the delta channel network and improve stratigraphic models of deltas.

INTRODUCTION

Given the importance of wetlands in protecting coastlines from storm surges (Danielsen et al., 2005; Costanza et al., 2006; Day et al., 2007) and maintaining a healthy ecosystem, there is considerable interest in coastal wetland restoration in the world's deltas (Michener et al., 1997; Smit et al., 1997; Valdemoro et al., 2007). Restoration plans commonly advocate a philosophy of restoring and taking advantage of the natural processes that create wetlands (United States Army Corps of Engineers, 2004; Reed and Wilson, 2004; Costanza et al., 2006). Most coastal wetlands are naturally created within the active delta channel network (Coleman, 1988; Day et al., 2000) as channels at the shoreline prograde basinward, bifurcate around river mouth bars (Bates, 1953; Wright, 1977; van Heerden and Roberts, 1988; Edmonds and Slingerland, 2007), and avulse to new locations (Coleman, 1988; Swenson, 2005; Edmonds and Slingerland, 2007; Jerolmack and Swenson, 2007; Hoyal and Sheets, 2009). The formation of deltaic bifurcations can already be predicted (Edmonds and Slingerland, 2007), but to restore and take advantage of the complete cycle in wetland restoration we need to understand what factors control the timing and location of deltaic avulsions.

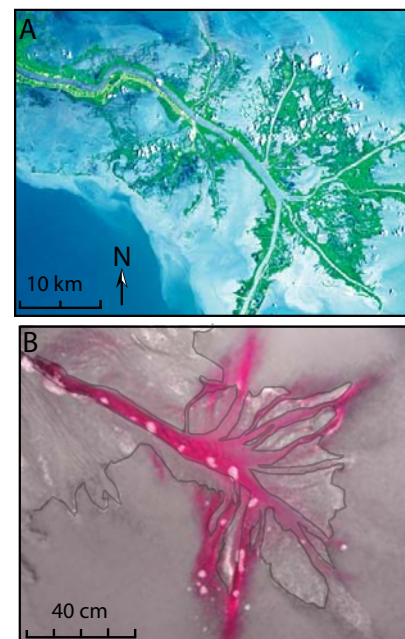
Delta avulsions occur across a variety of time and space scales. For example, on the Mississippi River, delta lobe switching originates at the apex of the delta approximately every 1 ka (Coleman, 1988), whereas intradelta lobe switching occurs within the active channel network approximately every 100 years (Coleman and Gagliano, 1964). Two of us suggested (Hoyal and Sheets, 2009), that the latter class of delta avulsions is controlled by downstream processes rather than upstream processes. In experimental deltas, we observed that an upstream-migrating flow disturbance creates flooding, which led to avulsion. However, the measurement technique (dye and overhead photos) did not allow quantification of how the flow disturbance propagates upstream and causes an avulsion, or when and where the avulsion occurs. Here we use novel experimental techniques to characterize the evolving bed and water surface in experimental deltas. We present a clear description of avulsion mechanics in intradelta lobes and demonstrate for the first time that the location and timing of downstream-controlled avulsions are predictable.

HYPOTHESIS AND METHODOLOGY

We test the hypothesis that intradelta lobe avulsions in homopycnal, river-dominated deltas are the result of two processes: distributary channel lengthening (the setup) and the growth of river mouth bars (the trigger). As the distributary channel within the intradelta lobe lengthens, a river mouth bar forms at its mouth and is recycled basinward. Eventually, the river mouth bar stagnates and triggers a period of increased bed aggradation and overbank flow upstream, that in turn leads to avulsion.

To test this hypothesis, we conducted physical scale-modeling experiments of delta systems in a 3×5 m tank of standing water with steady allogenic forcing. The boundary conditions consisted of steady, uniform sediment feed rate (18.2 g min^{-1}) and water discharge (10 L min^{-1}) entering into a basin (~ 4 cm depth) through a constant-width slot (0.038 m). The sediment mixture ranges from bentonite clay to coarse sand, and is combined with stabilizing polymer to reproduce the dynamics of fine-grained, cohesive deltas. The experimental deltas have higher slopes (mean bed slope is 0.02) than field-scale deltas. This does not affect our results because both along-channel and cross-levee slope are exaggerated equally. We infer that the processes in field-scale deltas are captured in experimental deltas because the network geometry of each delta is similar (Fig. DR1 in the GSA Data Repository¹), resulting in planview similarity (Fig. 1). Every process in field-scale deltas is not scaled; therefore these data are applicable to field-scale deltas only in a general sense. The deltas

Figure 1. A: 2001 Advanced spaceborne thermal emission and reflection radiometer (ASTER) image of Mississippi delta (courtesy of U.S. Geological Survey National Center for Earth Resources Observation and Science, and National Aeronautics and Space Administration Landsat Project Science Office). B: Overhead photo of experimental delta created with cohesive sediment mixture. White spots are foam on water surface.



¹GSA Data Repository item 2009182, Figures DR1–DR4 and Table DR1, is available online at www.geosociety.org/pubs/ft2009.htm, or on request from editing@geosociety.org or Documents Secretary, GSA, P.O. Box 9140, Boulder, CO 80301, USA.

created in this study are constantly at or above bankfull discharge and therefore represent evolution over many floods.

We produced four deltas under identical boundary conditions and collected data on ten intradelta lobes (labeled DL1, DL2, DL4, DL5, DL7–DL12). On each intradelta lobe we used a StarCam, which is a commercially available stereo camera with millimeter-scale horizontal and vertical resolution (Fig. DR2), to record the bed and water surface topographies at 20 min intervals until an avulsion occurred. To collect bed topography we turned off the water and sediment mixture entering the basin and then scanned the bed surface. After scanning we turned the water on, allowed the system to reequilibrate, and injected titanium dioxide to make the water opaque. We scanned the surface again, this time recording the water surface topography both within the channel and overbank. Of the ten lobes, two (DL10, DL11) will not be considered because they became entrenched against the tank wall and did not avulse. For a more detailed discussion of the methodology and scaling issues, see Hoyal and Sheets (2009).

AVULSION CYCLE IN DELTAS

Analysis of time-series photography and topography of the eight lobes shows a common sequence of morphodynamic events leading to avulsion and lobe abandonment (Fig. DR3). Initially, the distributary channel and the river mouth bar prograde with little to no bed aggradation along the channel ($t/t_a = 0-0.6$, where t is start of experiment, and t_a is initiation of avulsion; Fig. 2A). During progradation the river mouth bar enlarges, which leads to stagnation, aggradation of the bar to sea level, and splitting of the flow. The distance of river mouth bar progradation,

and therefore the length of the newly created intradelta lobe, is proportional to M , the jet momentum flux at the channel mouth, and inversely proportional to grain size to approximately the one-fifth power (Edmonds and Slingerland, 2007).

After river mouth bar stagnation, the bar is an obstruction that creates a local bow wave with decreased velocity near the bar, which causes bed aggradation immediately upstream of the mouth bar (Fig. 2A, location 1, $t/t_a = 0.6-1.25$). The aggradation immediately upstream of the river mouth bar then creates a new local bow wave even farther upstream that leads to local aggradation (Fig. 2A, locations 2 and 3, $t/t_a \sim 0.75-1.25$). This upstream-propagating bow wave, or “morphodynamic backwater” (Hoyal and Sheets, 2009), is a wave of bed aggradation and water-surface rise that causes a statistically significant increase (95% confidence level) in the net aggradation of the distributary channel network when compared to before mouth bar stagnation. In all the experiments, the net aggradation within the channel prior to mouth bar stagnation (Fig. 2B, $t_b/t_a = -0.5-0$ [t_b is the time when the river mouth bar stagnates]) is small. After mouth bar stagnation, the net aggradation increases sharply (Fig. 2B, $t_b/t_a = 0-0.5$) due to the upstream-propagating morphodynamic backwater.

As the morphodynamic backwater moves upstream, the channel bed aggrades, the water surface rises, and there is increased flow over the levees. In five experiments (DL 2, DL4, DL5, DL9, DL12) there is sufficient temporal resolution to resolve the change in overbank flow through time. In those experiments, the percentage of wetted levee initially remains relatively constant (Fig. 3A, $t/t_a = 0-0.7$). After the river mouth bar stagnates, the morphodynamic backwater moves upstream and the percentage of wetted levee increases significantly (Fig. 3A, $t/t_a \sim 0.7-1$) until an

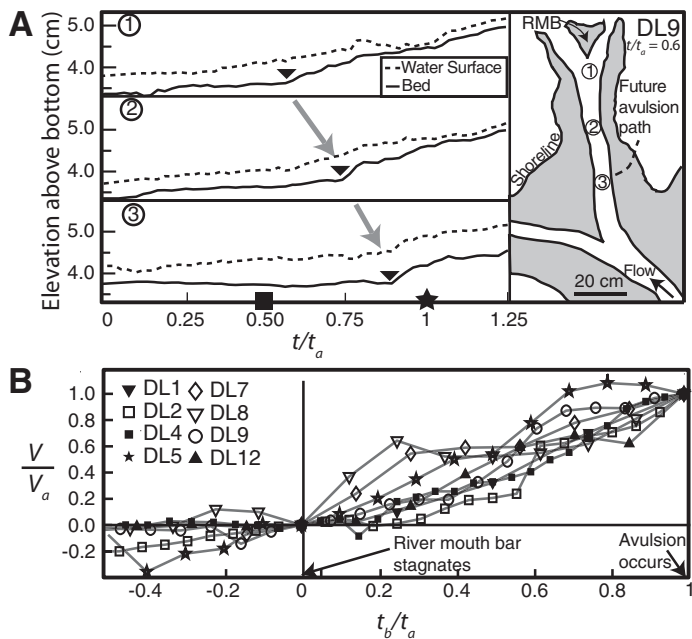


Figure 2. A: Time evolution of bed and water surface since start of experiment (t) relative to initiation of avulsion (t_a) for three locations marked on trace of DL9 shoreline. After river mouth bar (RMB) stagnates (square on x axis), bed begins to aggrade (marked by upside-down triangle) at location 1, and that change in aggradation propagates upstream to locations 2 and 3. Avulsion (star on x axis) is initiated at location 3 soon after morphodynamic backwater reaches that location. **B:** Time evolution of cumulative sediment volume (V) deposited within distributary channel relative to sediment volume deposited from RMB stagnation to avulsion (V_a). Timing of RMB stagnation (t_b) relative to t_a is defined as zero and therefore negative values represent times before RMB stagnation. Areal extent of channel used to calculate V and V_a was held constant for all experiments.

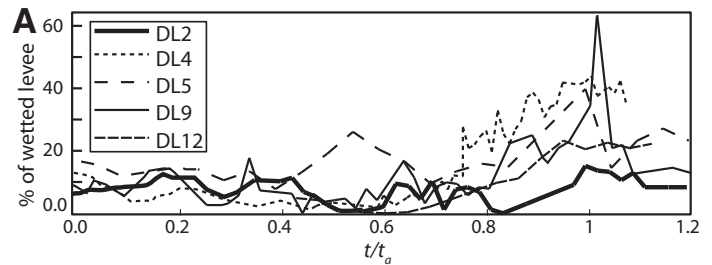
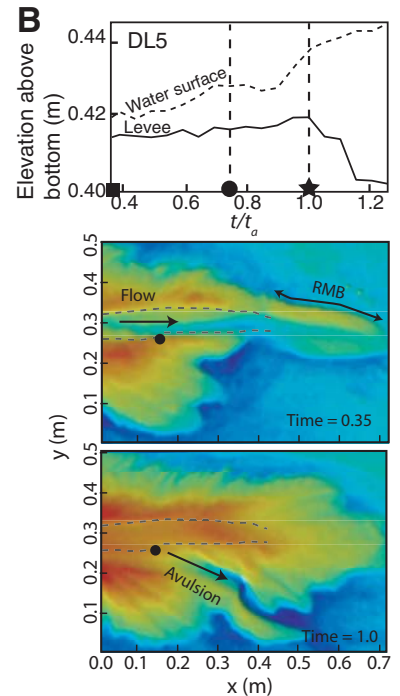


Figure 3. A: As morphodynamic backwater moves upstream, percentage of wetted levee length increases until avulsion is initiated at $t/t_a = 1$. Levee is defined as wetted if flow depth is >1 mm (Fig. DR2; see footnote 1). **B:** After passage of morphodynamic backwater (marked by circle in plot), water surface elevation over levee increases, levee top is eroded, and avulsion is initiated (marked by star). Passage of morphodynamic backwater wave was estimated by tracking change in bed aggradation as shown in Figure 2A. Circle on topographic maps marks location of position plotted. On topographic map, red and blue represent high and low elevations, respectively.



avulsion is initiated. After an avulsion is initiated, the percentage of wetted levee length begins to decline (Fig. 3A, $t/t_a > 1$) as the water-surface elevation in the now moribund channel decreases.

The cross-levee flow generated by bed aggradation during the morphodynamic backwater is a necessary condition for avulsion because avulsions are initiated only after its passage (Table DR1). For example, in DL5 (Fig. 3B), the levee and water surface elevation at the avulsion site remain constant until the morphodynamic backwater passes and the flow depth over the levee crest increases. The increased flow depth increases the bed shear stress and the levee begins eroding, leading to avulsion initiation. Avulsion initiation is defined as the point in time when the levee at the avulsion site begins to undergo runaway erosion (Fig. 3B, $t/t_a = 1$). Over the entire delta the amount of cross-levee flow is not spatially uniform, but depends upon levee heights and channel bed topography. For example, deep scour holes attenuate the aggradation signal of the morphodynamic backwater and keep the flow in bank, whereas shallower sections undergo more aggradation relative to flow depth and consequently show more overbank flow.

The location of the avulsion depends not only upon the magnitude of the shear stress on the levee crest, but also upon the duration of its application. We propose that avulsion location is governed by time-dependent processes, because there must be a large enough shear stress on a levee to begin erosion, and it must be exerted long enough to erode a crevasse and construct an avulsion channel across the floodplain. This time dependence suggests that the avulsion should occur where the cross-levee impulse per unit area of the flow, I ($\text{kg m}^{-1} \text{s}^{-1}$), is maximized:

$$I_i = \int_0^{\Delta T} \tau_i \cdot dt, \quad (1)$$

for all $\tau_i > 0$, where τ_i (N m^{-2}) is the bed shear stress at location i along the levee crest and ΔT (s) is total duration of cross-levee flow during the interval from river mouth bar stagnation until just prior to avulsion initiation. Assuming steady, uniform flow, τ equals ρghS , where h is the water depth of flow crossing the levee crest and S is the floodplain slope measured from the levee crest to the shoreline along the path of steepest descent. The variable I is a proxy of the potential total amount of sediment transported during ΔT . A plot of I at various points along the levee crest during ΔT (Figs. 4A and 4B) indicates that the avulsion occurs at the location of maximum I with 93% accuracy. In general, the location of I_{\max} is a characteristic distance upstream from the river mouth bar between 5 and 13 channel widths ($n = 8$), which is consistent with length scales of intradelta lobe avulsions in the Mississippi delta (Coleman and Gagliano, 1964). These sites are far enough upstream that the cross-levee slope is appreciable, but are far enough downstream so that flooding due to the morphodynamic backwater effect is sustained for a long time. Finding the location of I_{\max} can be used to predict the avulsion location because in all the experiments I_{\max} stabilizes near the avulsion site well before the avulsion occurs (Fig. DR4).

APPLICATION TO FIELD-SCALE DELTAS

These results provide guidelines for predicting avulsion locations on a delta, and the area and rate of creation of new wetlands associated with each avulsion. Even though antecedent conditions, such as irregular levee topography, previously channelized flow paths (Aslan et al., 2005; Jerolmack and Paola, 2007) and spatial variation of accommodation space, can influence the location of the avulsion, I_{\max} is still a reliable predictor of avulsion location. For example, in two experiments (DL2 and DL9) the location of I_{\max} is coincident with low average bed shear stresses on the levee, making those locations ostensibly poor candidates for avulsion. However, the partially channelized conditions of the floodplain adjacent

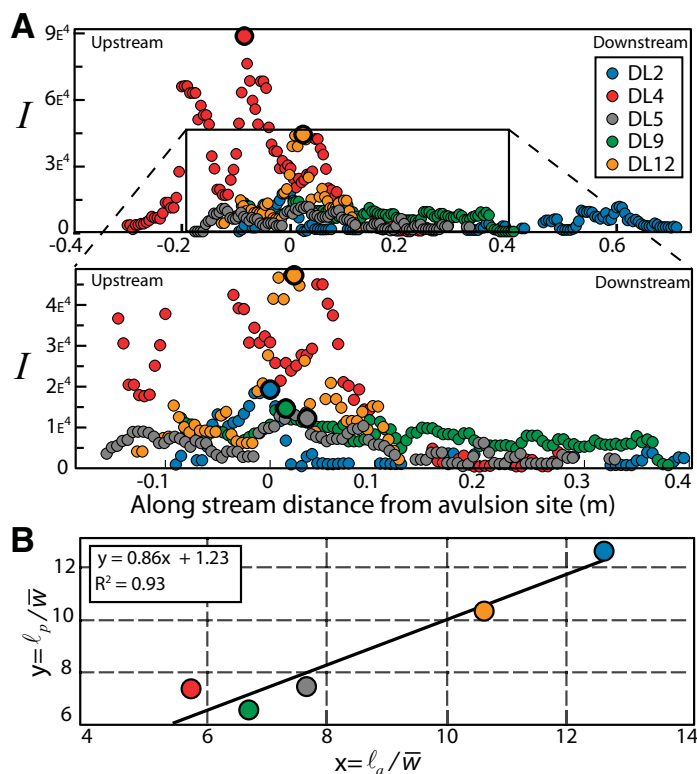


Figure 4. A: Avulsion occurs in space where I , the cross-levee impulse, is greatest (marked by larger dot). I_{\max} corresponds to location where greatest average shear stress has been applied for longest time. Each data point represents average shear stress on levees for one channel cross section and is averaged in time from river mouth bar (RMB) stagnation until one scan prior to avulsion. Channel cross sections are averaged over 1.5 cm swaths and are calculated every 1.5 cm. The x axis is shifted so that zero marks avulsion location for each experiment. **B:** Avulsion location (ℓ_a) can be predicted (ℓ_p) with 93% accuracy by finding location of I_{\max} (large dots in A). Avulsion distances are measured from RMB crest to avulsion location and non-dimensionalized by average channel width (\bar{w}) in time and space.

to those locations permitted removal of sediment transported overbank, which sustained overbank flow, thereby maximized I , and eventually facilitated the avulsion.

To determine the exact avulsion time and location, one must know the critical value of I_{\max} for levee failure, but even without that, the location of I_{\max} serves as a likely predictor of future avulsion location. The location of I_{\max} can be predicted on field-scale deltas by a number of techniques. A high-resolution topographic survey of a delta coupled with a morphodynamic numerical model would allow simulation of repeated flooding on the delta and thus determination of I_{\max} . Satellite measurements of water depth and water surface elevation (e.g., Alsdorf et al., 2007) collected during multiple floods could be used to estimate the location of I_{\max} . Predicting the location of I_{\max} could benefit wetland restoration strategies (Reed and Wilson, 2004) that rely on human-made crevasses (e.g., West Bay Sediment Diversion on the Mississippi delta) to create wetlands. Crevasses placed at locations of I_{\max} would more likely lead to sustainable wetlands because they are constructed near the site where the system would naturally create wetlands.

Once an avulsion is created at the location of I_{\max} , it is possible to estimate the future area and rate of wetland creation. Here we define wetlands as the partially inundated area of the intradelta lobe adjacent to the distributary channel and its levees (Fig. DR3). On experimental deltas in this study, the intradelta lobe length is a function of average intradelta lobe

width. Therefore, lobe area and wetland area can be predicted from the lobe length. As noted, lobe length is a function of the jet momentum flux at the river mouth, M . When an avulsion occurs, the area of future wetlands depends upon the location of I_{\max} because discharge increases up-delta, and therefore so does M .

The rate at which new wetland area is created depends upon the upstream-propagation speed of the morphodynamic backwater compared to the rate of river mouth bar construction. If the upstream propagation of the morphodynamic backwater is fast compared to river mouth bar construction, then avulsions occur quickly and tile the nearshore shallow water with intradelta lobes that evolve to wetlands. If the upstream propagation of the backwater is slow, then lobe construction will continue into deeper water, where less subaerial land is created per unit time because of the increased accommodation space. Therefore, in two delta lobes with the same M and I_{\max} , the lobe with a faster upstream propagating morphodynamic backwater will produce more wetland area per unit time.

The relative rates of the upstream propagation of the morphodynamic backwater and the construction of river mouth bars may also help elucidate controls on delta morphology. If the upstream propagation of the morphodynamic backwater is slow relative to river mouth bar construction, then the system will continue to prograde basinward and bifurcate via mouth bar deposition (e.g., Edmonds and Slingerland, 2007). If, on the other hand, the upstream propagation is fast compared to river mouth bar construction, then the avulsion process will dominate delta morphology.

CONCLUSIONS

Here we have used physical experiments to develop the first mechanistic model that describes the complete avulsion cycle in river-dominated deltas and allows prediction of avulsion location. The results clearly demonstrate that a class of avulsions is controlled by downstream processes, such as a growing river mouth bar, that cause an upstream migrating wave of bed aggradation and overbank flow. The avulsion timing and location can be predicted by finding the levee location that maximizes the product of shear stress and duration. To insure that the process of avulsion and wetland creation remains active in field-scale deltas, the dredging of distributary channels and river mouth bars should be minimized, because it disrupts the bed aggradation from the upstream-propagating morphodynamic backwater.

The extent to which the processes described in this paper actively participate in causing full-scale delta avulsions, which occur many channel widths upstream of the river mouth bar, remains an interesting question.

ACKNOWLEDGMENTS

We acknowledge funding from Exxon Mobil, National Science Foundation grant EAR-0809653, and the Donors of the American Chemical Society Petroleum Research Fund for support of this research. We thank R. Alley, J. Best, R. Bloch, J. Bridge, D. Hill, E. Kirby, C. Marone, D. Parsons, A. Rathbun, and N. Smith for useful discussions, and A. Aslan and C. Paola for insightful comments that strengthened this manuscript.

REFERENCES CITED

Alsford, D.E., Rodriguez, E., and Lettenmaier, D.P., 2007, Measuring surface water from space: Reviews of Geophysics, v. 45, RG2002, doi: 10.1029/2006RG000197.

Aslan, A., Autin, W.J., and Blum, M.D., 2005, Causes of river avulsion; insights from the late Holocene avulsion history of the Mississippi River, U.S.: Journal of Sedimentary Research, v. 75, p. 650–664, doi: 10.2110/jsr.2005.053.

Bates, C.C., 1953, Rational theory of delta formation: American Association of Petroleum Geologists Bulletin, v. 37, p. 2119–2162.

Coleman, J.M., 1988, Dynamic changes and processes in the Mississippi River delta: Geological Society of America Bulletin, v. 100, p. 999–1015, doi: 10.1130/0016-7606(1988)100<0999:DCAPIT>2.3.CO;2.

Coleman, J.M. and Gagliano, S.M., 1964, Cyclic sedimentation in the Mississippi River deltaic plain: Gulf Coast Association of Geological Societies Transactions, v. 14, p. 67–80.

Costanza, R., Mitsch, W.J., and Day, J.W., Jr., 2006, A new vision for New Orleans and the Mississippi delta: Applying ecological economics and ecological engineering: Frontiers in Ecology and the Environment, v. 4, p. 465–472, doi: 10.1890/1540-9295(2006)4[465:ANVFN0]2.0.CO;2.

Danielsen, F., Sorensen, M.K., Olwig, M.F., Selvam, V., Parish, F., Burgess, N.D., Hiraishi, T., Karunakaran, V.M., Rasmussen, M.S., and Hansen, L.B., 2005, The Asian tsunami: A protective role for coastal vegetation: Science, v. 310, p. 643, doi: 10.1126/science.1118387.

Day, J.W., Britsch, L.D., Hawes, S.R., Shaffer, G.P., Reed, D.J., and Cahoon, D., 2000, Pattern and process of land loss in the Mississippi Delta: A spatial and temporal analysis of wetland habitat change: Estuaries, v. 23, p. 425–438, doi: 10.2307/1353136.

Day, J.W., Jr., Boesch, D.F., Clairain, E.J., Kemp, G.P., Laska, S.B., Mitsch, W.J., Orth, R., Mashriqui, H., Reed, D.J., and Shabman, L., 2007, Restoration of the Mississippi Delta: Lessons from Hurricanes Katrina and Rita: Science, v. 315, 1679, doi: 10.1126/science.1137030.

Edmonds, D.A., and Slingerland, R.L., 2007, Mechanics of river mouth bar formation: Implications for the morphodynamics of delta distributary networks: Journal of Geophysical Research, v. 112, F02034, doi: 10.1029/2006JF000574.

Hoyal, D.C.J.D., and Sheets, B.A., 2009, Morphodynamic evolution of experimental cohesive deltas: Journal of Geophysical Research, doi: 10.1029/2007JF000882.

Jerolmack, D.J., and Paola, C., 2007, Complexity in a cellular model of river avulsion: Geomorphology, v. 91, p. 259–270, doi: 10.1016/j.geomorph.2007.04.022.

Jerolmack, D.J., and Swenson, J., 2007, Scaling relationships and evolution of distributary networks on wave-influenced deltas: Geophysical Research Letters, v. 34, L23402, doi: 10.1029/2007GL031823.

Michener, W.K., Blood, E.R., Bildstein, K.L., Brinson, M.M., and Gardner, L.R., 1997, Climate change, hurricane and tropical storms, and rising sea level in coastal wetlands: Ecological Applications, v. 7, p. 770–801, doi: 10.1890/10510761(1997)007[0770:CCHATS]2.0.CO;2.

Reed, D.J., and Wilson, L., 2004, Coast 2050: A new approach to restoration of Louisiana coastal wetlands: Physical Geography, v. 25, p. 4–21, doi: 10.2747/0272-3646.25.1.4.

Smit, H., van der Velde, G., Smits, R., and Coops, H., 1997, Ecosystem responses in the Rhine-Meuse delta during two decades after enclosure and steps toward estuary restoration: Estuaries and Coasts, v. 20, p. 504–520, doi: 10.2307/1352610.

Swenson, J.B., 2005, Relative importance of fluvial input and wave energy in controlling the timescale for distributary-channel avulsion: Geophysical Research Letters, v. 32, L23404, doi: 10.1029/2005GL024758.

United States Army Corp of Engineers, 2004, Louisiana coastal area (LCA), Louisiana, ecosystem restoration study: New Orleans, Louisiana, U.S. Army Corp of Engineers, 504 p.

Valdemoro, H.I., Sánchez-Arcilla, A., and Jiménez, J.A., 2007, Coastal dynamics and wetlands stability. The Ebro delta case: Hydrobiologia, v. 577, p. 17–29, doi: 10.1007/s10750-006-0414-7.

van Heerden, I.L., and Roberts, H.H., 1988, Facies development of Atchafalaya Delta, Louisiana; a modern bayhead delta: American Association of Petroleum Geologists Bulletin, v. 72, p. 439–453.

Wright, L.D., 1977, Sediment transport and deposition at river mouths: A synthesis: Geological Society of America Bulletin, v. 88, p. 857–868, doi: 10.1130/0016-7606(1977)88<857:STADAR>2.0.CO;2.

Manuscript received 15 December 2008

Revised manuscript received 27 March 2009

Manuscript accepted 2 April 2009

Printed in USA